

# Research on 3D Modeling of Wupaolong based on Sparse Point Cloud Reconstruction of SFM Algorithm

Jiantuan Huang

College of Physical Education and Health care, Guangxi University for Nationalities, Nanning, Guangxi, 530004, China

Lifang Huang

Leisure and Health College of Guilin Tourism University, Guilin, Guangxi, 541006, China

E-mail: 20020049@gxun.edu.cn

**Abstract.** As a classic project for the inheritance of Chinese folk culture, Wupaolong has the characteristics of unique material selection and complex production technology. However, as the finished products of folk handicrafts may not comply with production standards, a common problem in the production of handicrafts. Focusing on the problems of poor visual effects such as uneven surface and jagged edges in the craft paper binding model constructed by point cloud, and the need to enhance the sense of reality, this paper proposes an optimization method for 3D model and triangulation based on 3D line features. This method first preprocesses the feature points and performs sparse matching and dense matching on the processed feature points to generate a dense point cloud. The dense point cloud is then processed by an adaptive weighted median filtering method. This is followed by application of surface modeling method based on Delaunay algorithm to realize the reconstruction of object triangulation. Based on the triangular patch, the reference plane of the craft paper binding surface is fitted, and the model surface is corrected and optimized based on the reference plane. With the aid of three-dimensional line segments, the triangulation at the edge of the craft paper binding is corrected and optimized. Finally, an optimized three-dimensional model of craft paper binding is obtained. Experimental results show that the proposed algorithm can improve the unevenness of the 3D model plane and edges, and maintain the characteristics of the 3D model plane and edges. Compared with the existing surface reconstruction algorithms based on point cloud features, the optimized triangulation and model have higher accuracy and quality, which can greatly improve the visual effect of the model and improve the accuracy of the three-dimensional model. The research results of this paper can realize 3D modeling development for the production process of Wupaolong, effectively improve the elevation accuracy of the model, realize the production standard of digital Wupaolong model, and provide reference for folk production process. © 2022 Society for Imaging Science and Technology.

[DOI: 10.2352/J.ImagingSci.Technol.2022.66.3.030504]

## 1. INTRODUCTION

3D scene reconstruction is an important means of realizing the visualization of real 3D target information, and has been widely used in computer graphics, 3D printing, (Virtual Reality, VR), (Augmented Reality, AR) and allied fields, such as computer vision and photogrammetry, the contemporary themes of current research [1]. Recognizing from multiple

disciplines and perspectives that 3D printing is a key technology for the digital transformation of the economy and society, it will inevitably trigger a subversive change and prosperity in the inheritance and industrialization of folk sports culture. However, there are limited theoretical studies and empirical analysis on the characteristics and inheritance innovation of the new 3D printing in folklore sports industry, and the new industrialization characteristics of the folklore sports inheritance have not been systematically demonstrated. Moreover, there is a lack of overall awareness of the changes in the folklore sports industry making it difficult to explore effective innovation paths [2]. From the perspectives of industrial economics, network economics, and information economics, this paper takes the Binyang Firecrackers Dragon Festival as a national intangible cultural heritage. From 2007 to 2019, the Firecrackers Dragon Festival adopts methods such as questionnaire surveys, in-depth interviews, field visits, and participatory observations. We comprehensively comb the history of Firecrackers-Dancing Dragon industrialization, explore the integration between Firecrackers-Dancing Dragon and Internet technology, analyze the living context and contradictory characteristics of the 3D printing folk-custom competitive industrialization, and explore the inheritance and innovation path of the combination of digital economy and folk sports industry represented by 3D printing technology. All this can enhance the inheritance ability and effectiveness of folk sports culture.

Peng [3] et al. used the elevation point cloud data of the target as the object to study the information extraction and image post-processing of the three-dimensional target. By using a simple clustering method, the vertices of a plane with similar normal vector components are classified as a group of points on the same plane. The direction clustering method is used to divide each plane point, and the least square method is used to complete the data point fitting. This method establishes the outer boundary of the target facade, and then obtains the 3D coordinates of each corner point of the facade, and finally completes the 3D reconstruction of the target. This method can effectively improve the elevation accuracy of the target model. However, it uses all point cloud data to construct a three-dimensional target model, and the modeling method still has the problems of low efficiency and the overall accuracy of model reconstruction needs to

Received July 14, 2021; accepted for publication Nov. 14, 2021; published online Jan. 21, 2022. Associate Editor: Steven Simske.

1062-3701/2022/66(3)/030504/15/\$25.00

be improved. Chen [4] et al. proposed a novel point-based multi-view stereo (MVS) depth framework Point-MVSNet. This method first generates a rough depth map, converts it into a point cloud, and then refines the point cloud iteratively by estimating the residual between the depth of the current iteration and the true depth on the ground. The network effectively utilizes the three-dimensional geometric prior and two-dimensional texture information by fusing the three-dimensional geometric prior and two-dimensional texture information into the enhanced point cloud, and processes the point cloud to estimate the three-dimensional flow of each point. Experimental results prove that this point-based architecture has higher accuracy, higher computational efficiency and greater flexibility [5]. However, these methods rely solely on point clouds for modeling, and the modeling accuracy is still unsatisfactory in some cases and the edge accuracy and visual effects of the model are difficult to meet the needs of specific situations.

At present, due to the strict requirements of production cost and process inheritance, the production process of Wupaolong still remains at the level of manual production, and its production standard is only the overall sensory requirements of visual inspection, which can not be integrated with the advanced technologies such as 3D drawing, machining and 3D printing in the current information age. Therefore, it is difficult to inherit the production process and there is an urgent need for modern innovation in order to promote the maturity and development of dance gun dragon production technology in the new era.

According to the production process requirements of Wupaolong, the 3D line feature not only can be used to quickly model some scenes and requirements without high model accuracy and complexity, but also can optimize the craft paper binding model constructed from the point cloud to further improve the model accuracy and vision effect [6]. In view of the poor visual effects of Wupaolong point cloud model for the current craft paper binding, such as surface bumps and edge jaggedness, the existing model optimization methods make less use of line features, which leads to a situation where the optimization effect of the model with strong geometric features needs to be improved. This study first performs sparse matching and dense matching on the point cloud and generates a triangulated object network. Then, based on the triangular patch, the datum surface of the craft paper is fitted to correct and optimize the craft paper plane. Then the three-dimensional line segment is applied as an aid to correct and optimize the edge triangle net of the craft paper binding. Finally, the methods and strategies proposed in this paper are verified through comparative experiments.

The main innovations of this paper are:

A multi view matching method for oblique image line features under multiple constraints is proposed.

A fast reconstruction method of building 3D model based on inclined image line features is designed.



Figure 1. The physical model of Firecrackers-Dancing Dragon.

According to the Wupaolong model, the optimization method of building point cloud model based on line feature is established.

## 2. RELATED TECHNOLOGIES

### 2.1 *The Production Technology of Firecrackers-Dancing Dragon*

The production technology of Firecrackers-Dancing Dragon embodies the characteristics of locality, inheritance, variability and time. It regards local characteristics as its own personality and charm. The form of the production technology of the Firecrackers-Dancing Dragon is also changing, from the original closed technology to the family-style transformation [7]. The production technology of Firecrackers-Dancing dragon from the original liberation period, reform and opening to a harmonious society, unique and innovative production technology being the attraction and vitality, reflecting its theme of the times. In addition, the characteristics of the production technology of the Firecrackers-Dancing Dragon also reflect the characteristics of inheritance of national culture, showing national creativity, and enhancing national pride. The Firecrackers-Dancing Dragon model is shown in Figure 1:

The complexity of making the dragon head is that it is more difficult to make the mouth, beard and eye sockets. After the structure is finalized, it needs to be tied tightly with iron wire to take form. The head of Firecrackers-Dancing Dragon pays attention to simplicity, durability, firmness and lightness. Compared with making colorful dragons, there is no complicated appearance of colorful dragons, so there are relatively fewer processes. The dragon horns are made like deer antlers and tilted back slightly. The tongue is bent in a wavy shape with iron wire, and then it is floating in the

dragon's mouth. The bead is also made of iron wire and inlaid in the innermost part of the dragon's mouth [8].

## 2.2 Point Cloud Data Acquisition

The reconstruction of the 3D model of Firecrackers-Dancing Dragon based on photogrammetric images requires two steps, sparse reconstruction and dense reconstruction, which mainly involve two key technologies: SFM (Structure from motion) and MVS (Multi-view stereo). The SFM method performs camera pose estimation and sparse point cloud reconstruction, and the MVS algorithm is used to reconstruct the dense point cloud on this basis [9].

The SFM method extracts feature points from the image and performs matching to obtain feature points with the same name when the three-dimensional information and camera parameters in the scene are unknown. Using the principle of epi-polar geometry, the basic matrix is obtained from the feature point pairs of the two images with the same name. The three-dimensional information of the spatial point and the camera internal and external parameters of each image are calculated from the feature points with the same name on the image and the projection formula, and the sparse three-dimensional point cloud data and the camera parameters of each image are recovered from the image sequence. Finally, the beam adjustment is applied to optimize the parameters, and the triangulation method is used to restore the three-dimensional scene structure corresponding to these matching points from the feature points of the same name through the projection relationship [10].

Image matching based on the SIFT algorithm has high reliability, which is conducive to the subsequent surface reconstruction of the 3D model. However, it still belongs to feature point matching in essence, because feature points are usually sparse and unevenly distributed. The constructed 3D point cloud lacks necessary structural information, and it is difficult to express objects intuitively and be used for 3D model reconstruction. Existing methods usually use the method of region growth after the sparse feature points are obtained by matching or use the grid points of the regular divisions on the image to perform the subsequent dense matching [11].

## 2.3 Point Cloud Filtering

In the process of digital image acquisition, imaging, transmission and subsequent processing, due to the influence of internal and external factors such as non-target occlusion, mismatching, etc., gross errors and abnormal values will inevitably occur, and can result in image quality degradation, and it is so-called "noise" [12]. Commonly used plane fitting methods is considered, such as eigenvalue method, least square method. However, it is difficult to eliminate gross errors and outliers, and it is usually difficult to obtain satisfactory fitting results when there are a large amount of abnormal data in the data. According to the relationship between noise and image signal, noise types can be divided into additive noise and multiplicative noise. Among them, additive noise is more common, and the most typical ones

are Gaussian noise and impulse noise [13]. Before further processing the densely matched point cloud, it is a necessary to adopt appropriate methods to reduce the impact of noise. Among the current noise processing methods, the mean filter algorithm and the median filter algorithm are the two most commonly used methods.

### (1) Mean Filter Algorithm

The mean filter algorithm uses the average of the gray values of all pixels in a fixed filter template to replace the gray value of the central pixel in the neighborhood, as shown in formula (1):

$$g(x, y) = \frac{1}{M} \sum_{(x,y) \in S} f(x, y). \quad (1)$$

In formula (1),  $S$  is the collection of pixel coordinate points in the neighborhood of  $(x, y)$  points,  $M$  is the total number of pixels in the neighborhood,  $f(x, y)$  is the pixel of the original image, and  $g(x, y)$  is the pixel after the filter template is processed. The advantage of the mean filtering algorithm is that it is simple and easy to operate, but the disadvantage is that it is easy to lose the edge information of the image [14].

### (2) Median Filter Algorithm

The median filter algorithm is similar to the mean filter, the difference is that the median filter algorithm is used to replace the center pixel coordinates in the neighborhood instead of the average value. The central idea of the median filter algorithm is to sort and count the pixels in the neighborhood according to the gray level, and select the pixel with the gray value in the middle as the filtered output pixel [15]. The advantage of the median filter algorithm is that it can effectively suppress and eliminate noise when eliminating certain types of random noise, and the image boundary will not produce excessive blur. The disadvantage is that the size of the filter template of the traditional median filter algorithm cannot be changed according to the change of the noise concentration, and it is difficult to deal with the noise of the outermost pixel of the image [16].

According to different filter templates, the median filtering algorithm has two types: one-dimensional median filtering and two-dimensional median filtering. The one-dimensional median filter is shown in formula (2):

$$g(x, y) = \text{med} \{f(x - k, y - l), (k, l) \in W\}. \quad (2)$$

In formula (2),  $W$  is the filter template, and  $f(x - k, y - l)$  represents the gray value of the pixel in the template.

The two-dimensional median filter is shown in formula (3):

$$g(x, y) = \text{median}_{(x,y) \in S} \{f(x, y)\}. \quad (3)$$

In formula (3),  $f(x, y)$  represents the original image pixel, and  $g(x, y)$  represents the gray value of the pixel in the template.



Figure 2. The model structure of the Firecrackers-Dancing Dragon.

### 3. OPTIMIZATION IDEAS AND PROCESS OF 3D POINT CLOUD MODEL ASSISTED BY LINE FEATURES

The point cloud data acquired based on photogrammetry and computer vision methods are unevenly dense, and can result in uneven surface and jagged edges of the reconstructed 3D model, which is quite different from the real scene in terms of geometric consistency. Optimizing the object triangulation constructed from point clouds can further improve the accuracy and visual effects of the reconstructed model. However, most of the existing optimization methods only divide or deform the triangulation mesh to improve the triangulation mesh, and the optimization effect is limited. Besides, due to the complexity of the triangulation network, the model optimization efficiency is difficult to meet the requirements [17].

As is shown in Figure 2, focus is on the problems of poor object triangulation, poor model reality and model optimization methods in the current 3D model of Wupaolong based on point clouds, etc. The line feature is not sensitive to noise, has high structural stability, and has advantages in describing the structure and outline of the Firecrackers-Dancing Dragon target scene.

In this paper, an optimization method for 3D point cloud model of craft paper binding with the aid of 3D line features is proposed. The line feature is used in the optimization processing of the craft paper binding 3D model plane and the edge triangle net to improve the visual effect of the craft paper binding plane and edge, and improve the accuracy of the craft paper 3D model constructed by the point cloud [18]. The method flow is shown in Figure 3.

Firstly, the processing of image data mainly includes data preprocessing, sparse matching, dense matching, filtering and de-noising, and building a triangulation network. Secondly, the fitting and optimization of the model plane based on the triangulation of the object, mainly including the determination of the triangle planarity criterion, the determination of the adaptive threshold of the plane fitting, and the plane fitting and optimization based on the triangle surface. Finally, the model edge optimization and

correction based on line feature assistance mainly include the determination of three-dimensional line feature selection criteria, the determination of edge correction criteria, and the line feature-based edge optimization and correction [19].

This paper focuses on the following key aspects:

- (1) Determination of adaptive threshold based on line feature-assisted triangle patch fitting. By applying the idea of random sampling consistency to the process of plane fitting, three-dimensional line features are used as an aid to adaptively determine the threshold of plane fitting, in order to achieve the purpose of improving the efficiency of the algorithm and the degree of automation.
- (2) Model plane fitting and optimization based on triangular patches. Taking the topological relationship between the point clouds contained in the constructed triangulation network as a wedge machine, the plane fitting of the triangle surface of the triangulation network is performed and the plane of the three-dimensional model of Firecrackers-Dancing Dragon is optimized. It can improve the visual effect and reconstruction accuracy of the model plane, and maintain the geometric consistency of the model and the actual target.
- (3) Model edge optimization based on 3D line feature assistance. Through the acquired high precision and robust three-dimensional line segments and a series of correction criteria and energy functions formulated, the triangulation at the edge of the Firecrackers-Dancing Dragon model is optimized. Therefore, it can achieve the purpose of improving the visual effect and reconstruction accuracy of the edge of the model, and maintaining the geometric consistency between the model and the actual target [20].

### 4. THREE-DIMENSIONAL TARGET MODEL OF FIRECRACKERS-DANCING DRAGON BASED ON POINT CLOUD MODEL

#### 4.1 Constructing an Object Triangulation

The point cloud model is only a discrete sampling of the three-dimensional target model, which can only see the outline of the target surface, and cannot accurately and truly express the details of the target surface. Therefore, for the subsequent texture attaching and rendering work and better visual effects, it is necessary to use point cloud for meshing and transform the point cloud into a surface triangular mesh model that can be expressed mathematically [21]. The triangular mesh model is to construct the topological relationship between the sampling points after obtaining the geometric information of the dense or discrete sampling points on the surface of the target object. It uses a large number of triangular facets to form a piecewise linear triangular mesh surface, and then fits a solid approximation model. The model has flexible structure and good edge adaptability. It can represent a target entity with a more complex shape, and can obtain a three-dimensional surface model that meets different modeling requirements by controlling the number of triangular faces [22].

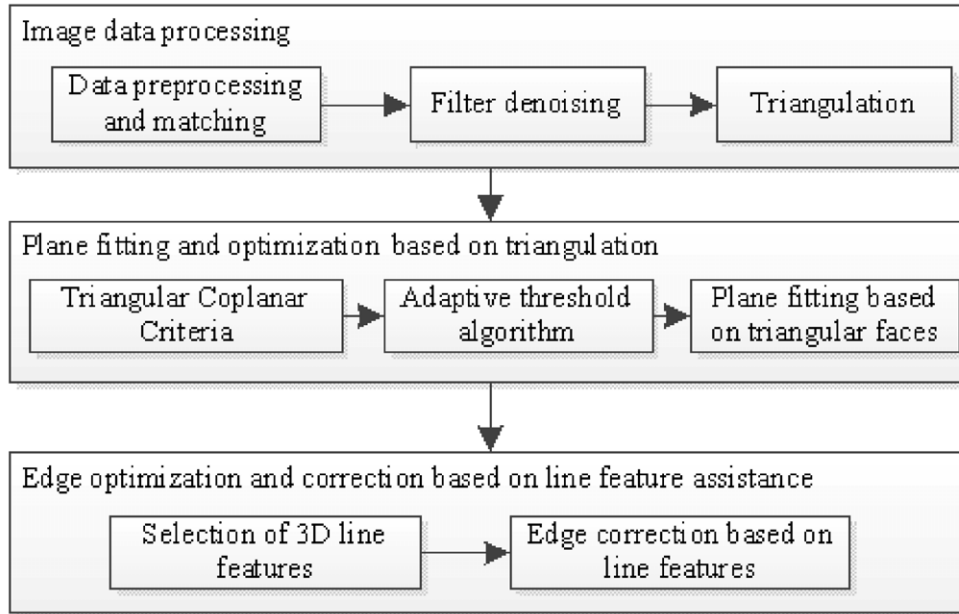


Figure 3. The basic process of the method in the paper.

The existing reconstruction methods of surface mesh model can be divided into three categories: The first category is reconstruction based on the Delaunay triangle algorithm. The main principle is to construct an initial seed triangle in the point cloud collection and continue to grow around it until all the data points are in a triangle network. The second category is the surface grid construction method based on implicit function. This method uses the difference of implicit function to fit the data, and then obtains the approximate surface. Its typical representative is the Poisson surface reconstruction algorithm. The third category is based on surface fitting methods [23]. This method uses simple geometric elements of specific shapes (such as planes, spheres, cylinders, etc.) to construct the entire surface geometry.

The Delaunay triangulation network and the Voronoi diagram have a dual relationship with each other, as shown in Figure 4.

As is shown in Fig. 4, set the discrete point  $S$ ,  $p_i$  is a 3D point.

The definition  $p_i \in S$  is shown in formula (4).

Supposing that discrete point set  $S$ ,  $p_i$  is three-dimensional points, where  $p_i \in S$ . The definition is shown in formula (4):

$$V(p_i) = \bigcap_{i \neq j} H(p_i, p_j). \quad (4)$$

where  $V(p_i)$  is called the Voronoi polygon about  $p_i$  or the Voronoi domain about  $p_i$ , which is closer to  $p_i$  than other points. The graph composed of the Voronoi polygons of all the points in the point set is the Voronoi diagram, and the triangular mesh formed by connecting all the points in the Voronoi diagram with the same side is the process of Delaunay triangulation. Delaunay triangle has

the characteristics of empty circle and maximum minimum angle, that is, the Delaunay triangulation has at most three points in a circle, and the circumscribed circle of any triangle does not contain other points. The possible triangulation formed by the discrete point set, the smallest angle of the triangle formed by Delaunay triangulation is the largest [24]. The Delaunay triangulation is defined as follows:

Assuming that  $V$  is a finite point set on a two-dimensional real number field, connecting two points  $a, b$  to form an edge  $e$ , where  $e \in E$ , then a triangulation  $T = (V, E)$  of  $V$  is a plane graph  $G$ .  $G$  satisfies the following conditions: The edge  $E$  in  $G$  only contains its own endpoints, there are no intersecting edges in  $G$ , all faces in  $G$  are triangles, and the set of faces is the convex hull of  $V$ . Delaunay triangulation means that a triangulation in  $V$  contains only Delaunay edges.

## 4.2 Optimization of Triangular Mesh

Triangular meshes can represent geometric models with complex topological structures and contours. However, they also have disadvantages such as large amount of data and poor smoothness. Meanwhile, the triangular mesh model obtained from the massive scattered data point cloud inevitably has various noises and outliers, which are difficult to use directly and cannot meet actual needs. Therefore, it is necessary to optimize the triangular mesh under the premise of ensuring the accuracy of the triangular mesh model to reduce data redundancy and de-noising. The existing various optimization methods of triangle mesh can be divided into topology optimization and geometric optimization [25].

### 4.2.1 Topology Optimization

The topological structure of the triangular mesh model can be divided into global topological structure and local

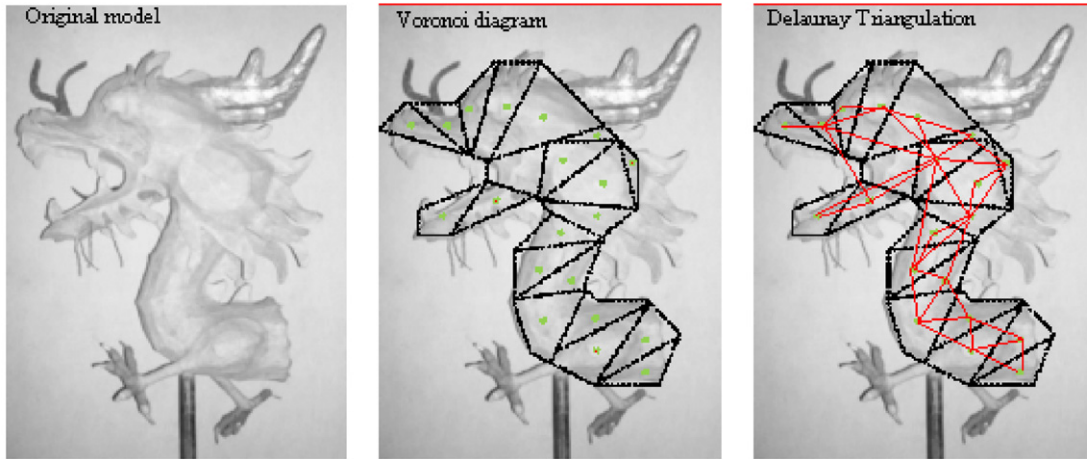


Figure 4. Voronoi diagram and Delaunay triangulation.

topological structure. Representing the overall geometric structure of the mesh model is called the global topology. Representing the geometric features around a vertex or triangle in the mesh model is called the local topology. Topology optimization mainly applies some rules such as the rule of side length and the rule of minimum angle and maximum. Under the condition of ensuring that the original data point set is fully or partially retained during the adjustment process, by operating on the edges or triangular patches, changing the local topological relationship of the mesh, that is, the connection mode of the triangular mesh nodes is changed to improve the mesh quality, where more typical methods are the minimum weight method and the minimum angle maximization method. The topology optimization method has high optimization efficiency and simple operation. However, because the shape change law of the model is not considered, the optimization effect is better in the flat area of the model, and the complicated part of the model or the part where the curvature changes drastically will cause large deformation, so the effect of improving the grid accuracy is poor [26].

In order to ensure that the new model is true and effective, it is usually necessary to impose certain constraints on the new model to ensure its rationality. When the number of triangles constituting the triangular mesh model is too large, it will undoubtedly take a lot of time to perform global optimization and adjustment of the triangular mesh model, and the algorithm efficiency is extremely low. Therefore, the original triangle mesh can be re-sampled as a whole. On the one hand, it can ensure that the triangles constituting the new model are relatively uniform, and on the other hand, the number of triangles in the model can be greatly reduced. Considering that the triangular mesh model does not have a fixed topological structure, it is difficult to perform overall re-sampling and smooth spline surface fitting. Therefore, it is necessary to divide the triangle mesh surface of any topology, so that the divided local area has a certain topological configuration, such as a three-boundary area, a four-boundary area, and so on.

#### 4.2.2 Geometry Optimization

Geometry optimization keeps the topological structure unchanged during the process of optimizing and adjusting the triangular mesh model. It mainly uses some algorithms to move, add or delete the positions of the vertices of the grid to minimize a certain geometric metric of the grid to achieve the purpose of changing the quality of the mesh. This method performs well in retaining the characteristics of the original model, but usually due to the complexity of the calculation process, the amount of calculation is large and the optimization efficiency is low. Meanwhile, it is easy to reduce the accuracy of the original point cloud data, and the geometric optimization can be subdivided into two types: the point addition method and the point shift method [27].

The point addition method improves the mesh quality by adding an appropriate amount of points to the poorly shaped triangular mesh, but it is usually difficult to ensure the convergence of the mesh and the rules for adding points are complicated. The point shift method achieves the purpose of optimizing the triangular mesh model by adjusting the geometric position of the vertices of the triangular mesh. Commonly used methods are the energy method and the Laplace method. The energy method combines the geometric and physical properties of the triangle mesh model, and uses all the triangle mesh vertices as parameters to define a global energy function for the original triangle mesh model. It adjusts the mesh vertices by constraining the minimum value of this function to solve, so that the overall energy function of the triangular mesh model under certain constraints is minimized. This method is computationally expensive and does not have an advantage in local shape control, but the optimization effect of triangle mesh is better [28].

The Laplacian method defines a Laplacian for each vertex in the triangular mesh, as shown in formula (5):

$$L(P) = \frac{1}{\sum_{j \in D(P)} w_j} \sum_{j \in D(P)} w_j Q_j - P. \quad (5)$$

In formula (5),  $D(P)$  represents a certain neighborhood of vertex  $P$ , and  $w_j$  is the weight of each point in  $D(P)$ .

Through iterative calculation, the vertices of the triangular mesh are moved to the centroid of the triangular facets formed by the units around the vertices along the direction determined by the Laplacian operator, so as to realize the optimal adjustment of the mesh, as shown in formula (6):

$$x_0^{\text{nev}} = x_0^{\text{old}} + \lambda \sum \left( \frac{x_i^{\text{old}} - x_0^{\text{old}}}{n} \right), 0 < \lambda < 1. \quad (6)$$

$L(P)$  is applied to the vertex  $P$ , the position adjustment formula of  $P$  can be obtained as formula (7):

$$P_{\text{new}} = P_{\text{old}} + \lambda L(P_{\text{old}}). \quad (7)$$

In formula (7),  $\lambda$  is a positive constant, which is used to control the speed optimization of triangle mesh.

This method is simple and fast to operate, but the disadvantage is that the influence of constraint conditions on mesh adjustment is not considered, which makes it impossible to optimize and improve the boundary triangle surface. The method cannot be applied to a mesh model with uneven distribution of triangles and a large number of irregular triangles [29].

## 5. OPTIMIZATION ALGORITHM OF 3D POINT CLOUD MODEL ASSISTED BY LINE FEATURE

Before the image data processing, the preprocessing of the image data should be carried out, which usually includes the steps of camera calibration and distortion correction, image resampling, uniform light and uniform color processing, and pyramid image generation. Camera calibration is used to calculate the internal orientation elements and distortion parameters of the camera, and use the calibration parameters to perform distortion processing on the image to eliminate system errors caused by internal system or environmental factors. Image resampling is used to interpolate to obtain the smooth transition of gray levels between sampling points, which is usually done by bilinear interpolation. Uniform light and uniform color processing is used to eliminate the differences in color, contrast, brightness and darkness between images caused by factors such as lighting conditions, CCD characteristics, and uneven optical lens imaging. The pyramid algorithm is used to decompose the original image into sub-images with different spatial resolutions to improve the efficiency and accuracy of matching [30].

### 5.1 Point Feature Matching and Dense Matching

Scale invariant feature transformation (SIFT), as a feature descriptor based on local invariants, has the characteristics of maintaining invariance to image scale and rotation, and strong adaptability to illumination changes and image deformation. Image matching based on SIFT features has the advantages of high accuracy, strong robustness, and fast speed. Therefore, this paper uses the SIFT algorithm to extract and match point features of the image.

After obtaining the sparse point cloud based on the SIFT algorithm, this paper adopts the dense matching method of CMVS (cluster multi-view stereo) and PMVS (patch-based multi-view stereo). The CMVS method is used to cluster and classify the image set to reduce the amount of data in the reconstruction process, improve the efficiency of dense matching, and increase the speed of calculation. Furthermore, the PMVS method can complete the final dense matching through three main steps: matching, expansion, and filtering.

In order to take into account the noise removal ability and the sparse point cloud in the texture sparse area, this paper adopts an adaptive weighted median filter method to process the densely matched point cloud. This method can assign different weights to the pixels according to the change of the filter window size, in order to eliminate the noise without reducing the distortion of the image details, and lay a good foundation for the subsequent triangulation construction. The central idea of the algorithm is to define a window to slide on the image to detect noise points and then to count the number of noise points and adjust the filter size of the window. Finally, it assigns a corresponding weight to each pixel in the neighborhood according to a predefined function, and use the weighted gray value as the output value of the final filtering process. The weighting algorithm is defined as shown in formula (8):

$$y = \text{med}\{w_1x_1, w_2x_2, w_3x_3, \dots, w_Nx_N\}, \quad (8)$$

where  $(x_1, x_2, x_3, \dots, x_N)$  is the gray value of the pixel in the filter window, the window size is  $W_N (N = (2n + 1) \times (2n + 1))$  and  $(w_1, w_2, w_3, \dots, w_N)$  is the corresponding weights, and  $y$  is the output value of the window containing noise after filtering. This method can effectively combine the advantages of adaptive window and center weighting algorithm to accurately classify signal points and noise points, improve the filtering performance and effectively smooth the image. The most critical part is noise detection, which can be divided into the following two steps:

(1) a window  $f(x, y)$  centered on the pixel  $W_N (N = (2n + 1) \times (2n + 1))$  is created, it is slid on the image, all the pixels are sorted in the window, and the median  $I_{\text{med}}$ , maximum  $I_{\text{max}}$ , and minimum  $I_{\text{min}}$ , the average value  $I_{\text{mean}}$  of the pixel are found, as shown in formula (9):

$$\begin{aligned} I_{\text{med}} &= \text{median}\{f(x+i, y+j) | i, j = 1, \dots, n-1, n\}, \\ I_{\text{mean}} &= \frac{1}{N} \sum_{i=-n}^n \sum_{j=-n}^n f(x+i, y+j). \end{aligned} \quad (9)$$

If the central pixel is an extreme point and meets  $|f(x, y) - I_{\text{med}}| > d_{i,j}$ , the pixel is judged to be a suspected noise point, otherwise the filter size is expanded and noise detection is continued. If the center point still does not meet the condition when  $N = N_{\text{max}}$ , it is judged as a signal point,

as shown in formula (10):

$$d_{i,j} = \frac{1}{3} \sqrt{\sum_{i=-n}^{i=n} \sum_{j=-n}^{j=n} [f(x+i, y+j) - I_{\text{mean}}]^2},$$

$$\text{noise} = \begin{cases} 1 & |f(x, y) - I_{\text{med}}| > d_{i,j} \\ 0 & |f(x, y) - I_{\text{med}}| \leq d_{i,j}. \end{cases} \quad (10)$$

In formula (10),  $d_{i,j}$  is the threshold of the noise sensitivity coefficient based on the human eye.

(2) After the first step of detection, the pixels in the image are divided into signal points and noise points.

The noise points are processed by a weighted median filtering method. The gray value of the signal point pixel remains unchanged. According to the correlation of pixels in the image neighborhood, the expression definition of similarity is shown in formula (11):

$$g(x, y) = \sum_{(x,y) \in W_N} w(x, y) f(x, y), \quad (11)$$

where  $w(x, y)$  is the corresponding weight of the pixel in the filter window,  $f(x, y)$  is the pixel in the filter window, and  $g(x, y)$  is the gray value of the pixel in the window after filtering.

The mathematical expression definition of pixel weight is shown in formula (12):

$$w(i, j) = \frac{1}{\sum_{(i,j) \in W_N} \frac{1}{1 + (I(i, j) - I_{\text{mean}})^2}}. \quad (12)$$

### 5.2 Construction of the Object Triangular Network

The triangulation obtained by the Delaunay triangulation algorithm has the uniqueness of the result and the generated triangulation has good shape characteristics. Therefore, this paper adopts a surface modeling method based on Delaunay growth algorithm to realize the reconstruction of the object triangulation. The steps of the Delaunay growth algorithm in this paper:

- (1) All the points in the set NN are traversed, any two points are chosen and the distance DDD between the two points is calculated. The two points  $P_1$  and  $P_2$  with the smallest distance are selected from all distances to form the initial edge  $e_1$ .
- (2) The midpoint  $O$  of  $e_1$  is used as the starting point, the method of step (1) is applied to find the point  $P_i$  closest to  $O$ . Since the intersection of the three vertical bisectors is the center of the circumscribed circle, the center coordinates  $(x_0, y_0, z_0)$  of any three-point circumscribed circle can be calculated.
- (3) The circumscribed circle is judged. If the circle contains other points, step (2) is performed until no other points are included in a certain circumscribed circle. At this time,  $P_i$  is the optimal expansion point, so the initial triangle is constructed.

- (4) Based on the initial triangle, search for points that can form a triangle with each side of the initial triangle. Each edge grows up to two times and the expansion point must be in the direction of growth of the edge. The growth direction is calculated as shown in formula (13):

$$\vec{S} = \vec{AB} \times \vec{AD}. \quad (13)$$

If  $\vec{S} > 0$ ,  $D$  is on the left of  $\vec{AB}$ ; if  $\vec{S} < 0$ ,  $D$  is on the right of  $\vec{AB}$ ; if  $\vec{S} = 0$ ,  $D$  is on  $\vec{AB}$ .

- (5) The best points are selected from the candidate set, and the methods in steps (2) and (3) are used to construct a new triangle according to the principle that each side can only grow twice.
- (6) Steps (3)–(5) are repeated until all points form a triangular grid.

## 6. PLANE FITTING AND OPTIMIZATION BASED ON THE TRIANGULAR PATCH MODEL

### 6.1 Plane Fitting based on Triangular Patches

Compared with the point cloud data obtained by a three-dimensional laser scanner, the point cloud obtained by photogrammetry or computer vision methods has defects such as insufficient density and accuracy, and uneven density. Therefore, the existing surface reconstruction algorithms usually have uneven surfaces such as pits and bumps when generating the object triangulation, which leads to a certain difference between the reconstructed 3D model and the real scene in terms of geometric consistency.

The random sampling consensus algorithm is the RANSAC (Random Sample Consensus) algorithm, which mainly eliminates the influence of outliers or gross errors through random sampling, and constructs a sample subset consisting only of intra-office data. Algorithms usually first design judgment criteria for specific problems, use the judgment criteria to iteratively eliminate data that does not meet the parameter requirements, and then estimate the final parameters through the correct data set. It requires a certain confidence probability to support the minimum sampling number  $M$  of the sample subset and the probability  $P$  to obtain at least a subset composed of interior points. Its probability satisfies the relationship as shown in Eq. (14):

$$P = 1 - (1 - (1 - \varepsilon)^m)^M, \quad (14)$$

where  $\varepsilon$  is the data error rate, and  $m$  is the minimum number of data required to calculate the model parameters.

As an effective robust estimation algorithm, RANSAC algorithm has been widely used in the fields of feature matching, matrix estimation, model selection and so on. However, the existing plane estimation based on the RANSAC algorithm mostly uses all points indiscriminately for sample estimation, which is not only computationally intensive but also susceptible to error interference. The object-side triangulation is usually a Delaunay triangulation that is reconstructed after filtering and de-noising on the object-side point cloud obtained by dense matching. The

Delaunay triangulation network is not only reasonable and accurate, but also contains the correct topological relationship between adjacent object points. The correct topological relationship can effectively reveal the shape and topological structure of the surface of the object hidden in the point cloud data set.

Therefore, considering the topological connection between adjacent triangular facets and the overall smooth consistency, this paper combines the RANSAC idea to extract and fit the surface of Firecrackers-Dancing Dragon based on the reconstructed triangulation. Each triangle surface element in the triangulation network is used as a reference surface element, and whether a certain triangle surface element is coplanar with the reference surface element is used as a criterion for determining whether it is an interior point. It is used to find the sample subset with the largest number of interior points as the optimal plane fitting scheme. The basic process is as follows: select a certain triangle face element in the triangulation network as the reference face element, and the other triangle face elements are the set to be searched. In the set to be searched, starting from the adjacent triangular facets, from near to far in turn, determine whether other triangular facets are coplanar with the reference facet according to certain criteria. If they are coplanar, add the face element to the interior point set and remove it from the remaining searchable sets. If they are not coplanar, they are directly removed from the remaining searchable set, and the judgment of the next facet is continued. It can be seen from formula (14) that the lower the sample data error rate, the higher the probability of obtaining at least a subset composed of interior points, and the fewer sampling times required. After filtering, the rough points in the point cloud have been eliminated, and the triangulation network constructed by it can be regarded as a sample with a low data error rate. Therefore, after randomly sampling a certain number of interior point sets that meet the threshold condition, the sampling and iterative process can be terminated to improve the efficiency of the algorithm.

In order to avoid the influence of errors and obtain a robust plane fitting result, the method in this paper does not directly use the set with the largest number of interior points for plane fitting. Instead, the number of interior points corresponding to each reference panel is sorted, and the three corresponding to the most interior points are selected. Reference facets are based on the 9 vertices of the three reference planes, the least squares plane fitting is performed to obtain the final fitted reference plane. The schematic diagram of plane fitting based on triangle surface element is shown in Figure 5.

In Fig. 5, where the dotted line panel is the reference panel, the solid line panel is the “inner point” panel that is coplanar with the reference panel, and the yellow panel is the “outer point” panel that is not coplanar with the reference panel.

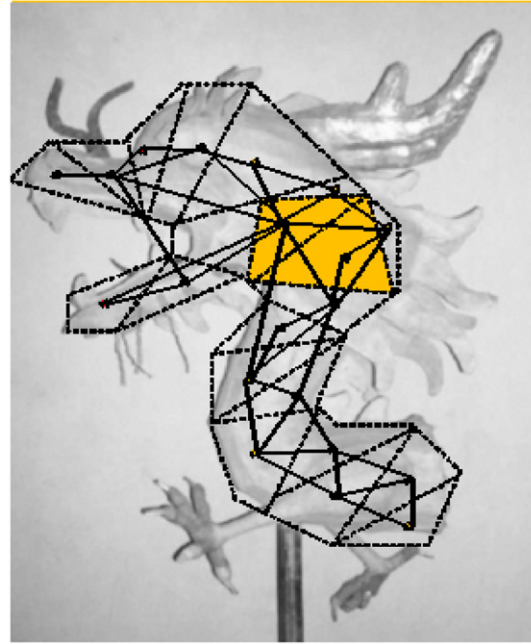


Figure 5. Plane fitting based on triangular patches.

### 6.2 Design of Judgment Criteria and Adaptive Threshold Function

In the algorithm proposed in this paper, selection method of the appropriate parameter model and the subsequent judgment criteria for determining whether two triangular facets are coplanar are particularly critical. The threshold used to separate the interior and exterior points is also very important. Since the modeling object in this article is craft paper tie, and most of the craft paper tie has a regular geometric shape and most of the turns are right angles, its contour lines usually have only two directions and are perpendicular to each other. Therefore, its surface can be treated as a plane. Generally speaking, the coplanar three-dimensional points satisfy formula (15):

$$ax + by + cz = d. \quad (15)$$

In the formula,  $(x, y, z)$  is the three-dimensional space coordinates of the object on the plane,  $(a, b, c)$  is the unit normal vector of the plane and satisfies  $a^2 + b^2 + c^2 = 1$ ,  $d$  is the distance from the origin of the coordinates to the plane. The distance from the three-dimensional point  $P(x, y, z)$  to the plane  $N$  is shown in formula (16):

$$d(P, N) = |ax + by + cz - d|. \quad (16)$$

Therefore, in this paper, the angle between the reference panel and the unit normal vector of the search panel  $\theta$  and the distance difference between the origin of the coordinates and the two facets  $\Delta d$  are used as the criterion for judging whether the two triangular panels are coplanar. The two facets elements need to meet two conditions to be coplanar: (1) The normal vectors of the two face elements are parallel or the included angle is less than a certain threshold. (2) The distance between the origin of the coordinate and the two

facets is equal or the absolute value of the distance difference is less than a certain threshold:

$$\theta = \cos^{-1} \frac{(\vec{n}_1 \cdot \vec{n}_2)}{|\vec{n}_1| \times |\vec{n}_2|}. \quad (17)$$

In formula (17),  $\vec{n}_1$  and  $\vec{n}_2$  are the unit normal vector of two facets. The distance difference is  $\Delta d = |d_1 - d_2|$ , where  $d_1$  and  $d_2$  are the distance from the origin of the coordinate to the two facets.

The angle between the normal vectors of the two facets is 0 and the distance difference between the origin of the coordinates and the two facets is 0. However, due to the influence of errors and actual operation, it is usually necessary to set a certain threshold  $\delta$  to approximate the tolerance value of the judgment criterion. The threshold includes two aspects: the normal vector included angle threshold  $\delta_1$  and the point-to-plane distance threshold  $\delta_2$ . When the angle between the normal vectors of the two facets is less than  $\delta_1$ , and the distance difference between the coordinate origin and the two facets is less than  $\delta_2$ , the search facet is classified as an interior point, otherwise it is an exterior point. In which the selection of the point-to-plane distance threshold  $\delta_2$  is particularly important. If the threshold is too small, the judgment will be too strict, and the effective points that should have been selected will be eliminated, resulting in the reduction of the plane range. If the threshold is too large, the error point or invalid point will be misjudged as a valid point, and the corrosion effect of the plane will be increased.

Generally, the threshold is determined by the researcher based on the actual situation. The algorithm in this paper adopts an adaptive threshold determination strategy, without artificially setting parameter thresholds, which reduces the workload and improves the degree of automation of the algorithm and the accuracy of the results.

### 6.3 Optimization of Plane Fitting based on Triangular Patches

Most of the existing model reconstruction methods are based on triangulation for surface reconstruction, and the final model surface is composed of triangulation. Because it has not been optimized, there are usually pits and bumps, and the surface is not smooth, which affects the visual effect of the model and the actual model accuracy. For craft paper binding, the surface of the model can be directly regarded as a flat plane without considering further refined modeling. Therefore, this article optimizes the object triangulation and plane because of the fitting plane.

After fitting the datum plane, all points on the plane should be on the datum plane, so all vertices on the triangle net are assigned to the plane. The vertices of the triangulation mesh are vertically projected to the reference plane, and the vertices of the triangulation mesh are driven to move along the projection direction to the reference surface, which can minimize the matching cost, realize the optimization of the

mesh, and obtain a flat plane composed of the triangulation mesh. As shown in Figure 6.

In Fig. 6, the triangulation mesh point  $P$  is corrected to the plane  $N$  along the direction of the projection line and becomes the point  $P'$ , and its constraint energy function is shown in formula (18):

$$E_S = \sum_{i=1}^m (P_i - P'_i), P_i \in \{R\}. \quad (18)$$

In formula (18),  $P_i$  is the coordinate of the mesh point to be corrected,  $P'_i$  is the coordinate of the projection point of the point on the datum plane, and  $m$  is the number of vertices of the triangle to be corrected.

## 7. OPTIMIZATION OF MODEL EDGES BASED ON 3D LINE FEATURE ASSISTANCE

The model reconstructed by the existing algorithm is not only flat enough on the surface, but also prone to severe jagged edges and sharp, which results in the model accuracy being difficult to meet the requirements and the visual effect, and it is a big difference in geometric consistency with the actual target features.

The algorithm in this paper uses the reconstructed high-precision and robust three-dimensional line segment as an aid, regards it as the three-dimensional manifestation of the actual target object edge, corrects the vertices of the triangle network near the edge, so as to improve the visual effect of the model edge and improve the modeling accuracy.

### 7.1 Acquisition of Three-dimensional Datum Line

Three-dimensional line segments are searched around the object triangle. If the three-dimensional line segment is a real and meaningful three-dimensional body at the edge of the model, the three-dimensional line segment should be located in a certain neighborhood of the triangulation network. The closer the distance, the higher the reliability and robustness of the three-dimensional line segment, the longer the line segment is considered to have no connection with the edge of the triangulation network. Therefore, the projection distance from the vertex of the triangulation net to the three-dimensional line segment should be less than a certain threshold. If there is no three-dimensional line segment in a certain neighborhood around a triangle grid, but the extension of a three-dimensional line segment is located in the neighborhood of the triangle grid, the three-dimensional line segment is also regarded as the reference line for triangle grid correction. The 3D mesh vertex is projected to the extension line of the 3D line segment, and the vertex is corrected to the extension line of the 3D line segment, so that can reduce the dependence of the model optimization on the accuracy of the edge end point of the craft paper binding. If there are multiple line segments around the triangular mesh, the projection distance from the vertex of the triangular mesh to each line segment is calculated separately, and the line segment with the smallest projection distance is selected as the correction reference line. If there is no three-dimensional

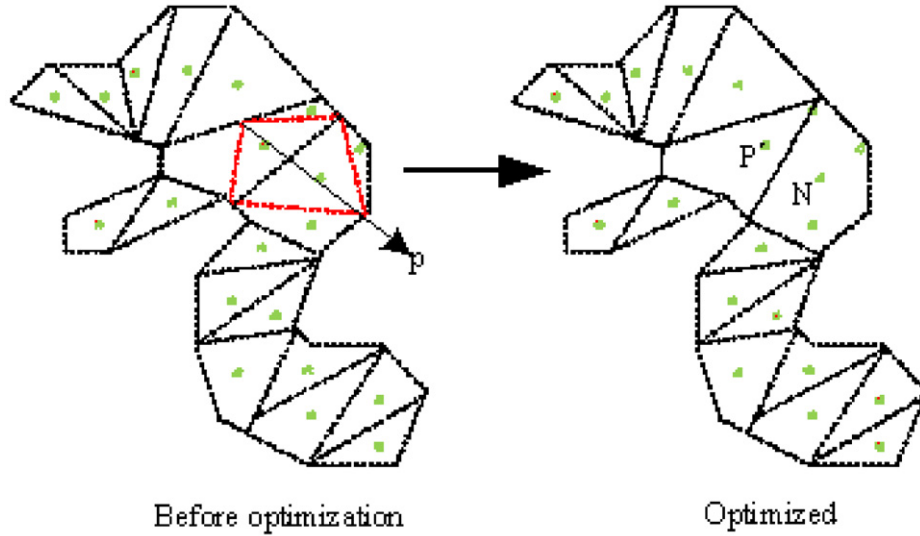


Figure 6. Optimization of triangular patches.

line segment around the triangulation, two points on the model are manually selected as the end points of the line segment, and the selected three-dimensional line segment is used as the reference line for subsequent triangulation correction.

### 7.2 Edge Optimization based on 3D Line Feature Assistance

After determining the triangle grid to be corrected, the mesh points are respectively projected to the nearest three-dimensional line segment, and the distance from the mesh point to the projection point is calculated. If the distance is less than the threshold, the mesh points are corrected to the three-dimensional line segment along the direction of the projection line. During the correction process, in order to ensure that the corrected triangulation network shape has no long and narrow triangles. The three vertices of the triangulation can be corrected at the same time, but they cannot be corrected to the same three-dimensional line segment. When the three vertices of the triangle mesh can and only can be corrected to a three-dimensional line segment, the vertex of the triangle mesh that is farthest from the three-dimensional line segment is removed from the points to be corrected, and no correction is made. Supposing that the grid point set to be corrected is  $\{R\}$ , and the energy function defining the three-dimensional line segment constraint is shown in formula (19):

$$E_l = \sum_{i=1}^n (p_i - q_i), p_i \in \{R\}. \quad (19)$$

In Eq. (19),  $p_i$  is the coordinate of the grid point to be corrected,  $q_i$  is the projected point coordinate of the point on the nearest three-dimensional line segment, and  $n$  is the number of vertices of the triangulation. For mesh points that are difficult to correct, the energy function is set to 0.

After correction, the mesh vertex near the 3D line segment is corrected to the nearest 3D line segment, and the edge of the model is also corrected into a straight line, as shown in Figure 7.

In Fig. 7, the thick black line is the reference line of the three-dimensional line segment,  $\beta$  is the distance threshold, the black points are grid points that are difficult to correct, and the red points are grid points to be corrected. The green dots belong to the triangle network to be corrected, but the mesh points are eliminated in order to avoid the appearance of long and narrow triangles after correction.

## 8. EXPERIMENTAL VERIFICATION AND ANALYSIS

In order to verify the effectiveness and feasibility of the method in this paper, the presented model is compared with the traditional point cloud-based Poisson surface reconstruction model in the three-dimensional visual effect of Firecrackers-Dancing Dragon. The Poisson surface reconstruction method is a more classic 3D modeling method based on point clouds. It has strong anti-noise interference ability and can adapt to the needs of 3D modeling in the case of low point cloud accuracy. Choosing the Poisson algorithm as a comparative experiment has a good sense of domain identity.

The RIEGL three-dimensional laser scanning system is used to scan the survey area, and the resolution of the point cloud obtained by scanning reaches 5 cm, and the laser point cloud is evenly distributed. The Firecrackers-Dancing Dragon point cloud obtained is used as the real model. The optimized model in this paper and the model constructed by the Poisson surface reconstruction algorithm are analyzed and compared with the real model. The flatness of the model surface is used as a quantitative evaluation index to verify the robustness and effectiveness of this method in improving the accuracy of the model. The flatness of the edge of the model is applied as a quantitative evaluation index to verify

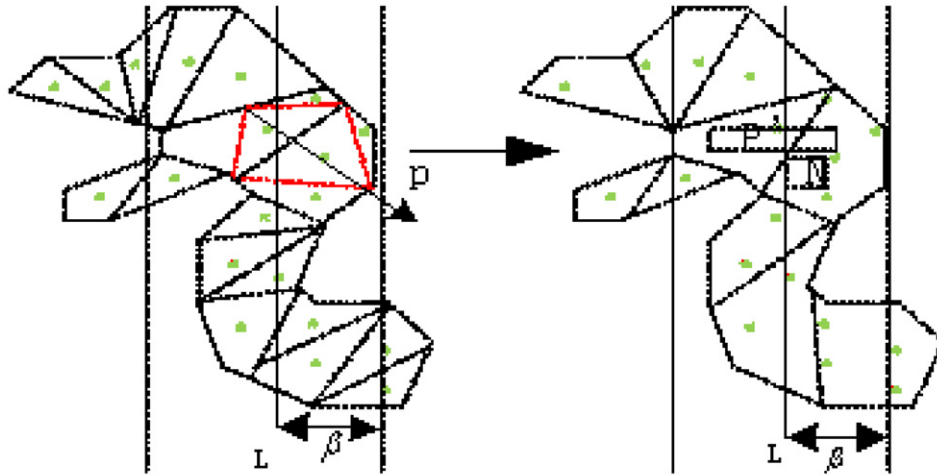


Figure 7. Optimization of edge triangulation assisted by line features.

the robustness and effectiveness of the method in this paper in improving the accuracy of the edge of the model.

About 1358 3D line segments are effectively extracted and reconstructed. However, due to various factors in line feature extraction and matching, the distribution of three-dimensional line segments is unbalanced. Not all edge triangulations can be optimized. Only the edges with three-dimensional line segments in a certain neighborhood around the edge triangle network can be optimized, and the proportion of triangle facets participating in the optimization is about 20.3%.

### 8.1 Comparison of Visual effects of Model Optimization

This paper optimizes the surface mesh construction method based on Delaunay triangulation. The proposed method is compared with the three-dimensional model of Firecrackers-Dancing Dragon constructed by the traditional point cloud-based Poisson surface reconstruction method, and the plane and the edge are analyzed separately. Due to limitations of available data conditions and time, no large-scale experimental verification has been carried out, and only experiments have been carried out on the point cloud of the paper dance cannon dragon. Besides, the focus of this article is on the optimization of details, only some models are selected before and after optimization as shown in Figure 8.

In Fig. 8, the plane model before model optimization is relatively clear, but there are traces of coarse dryness in the part with high eye curvature. For the optimized eye model, the texture model can obviously feel that the meshed model is more refined after refinement.

### 8.2 Accuracy Verification of Model Optimization

Two horizontal planes and vertical planes are randomly selected from the models obtained by the two methods, and 10 points are randomly selected on each plane to ensure the representativeness of the matching results. The distance is calculated between the selected points on each surface and the cloud-fitting plane of laser point, the standard deviation of the distance is used as the evaluation index of the “flatness”

of the model surface, and the average distance is applied as the evaluation index to optimize the plane accuracy of the model. It is stipulated that the plane of the point cloud fitting is used as the reference, the distance away from the model is positive, and the opposite direction is negative. In the same way, two horizontal edges and vertical edges are randomly selected from the models obtained by the two methods, and 6 points are manually selected randomly on each edge to ensure the representativeness of the matching results. The distance is calculated from the selected point on each edge to the laser point cloud fitting edge (20 cm from the center line of Firecrackers-Dancing Dragon edge). The standard deviation of the distance is used as the evaluation index of the “flatness” of the model edge. The average distance is used as the evaluation index of the edge accuracy of the optimized model. It is stipulated that the edge of the point cloud fitting is used as the reference, the distance away from the model is positive, and the opposite direction is negative. The unit of distance is cm. When calculating the mean and standard deviation, the distance is taken as the absolute value. The statistical results of the optimization accuracy of the model plane are shown in Table I.

Figure 9 shows the results of selecting a horizontal and vertical plane for each of the two models.

The test results in Table I and Fig. 9 have proved that the average distance between the overall model of the method and the real point cloud model is 3.245 cm, and the average distance from the overall model obtained by the Poisson algorithm to the real point cloud model is 5.429 cm. This algorithm has good processing effect.

The statistical results of the optimization accuracy of the model edges are shown in Table II.

Figure 10 shows the results of selecting a horizontal and vertical edge for each of the two models.

### 8.3 The Efficiency Experiment of the Algorithm

In the same experimental environment, using the same data source, three-dimensional modeling is carried out using the optimization method in this paper, the Delaunay

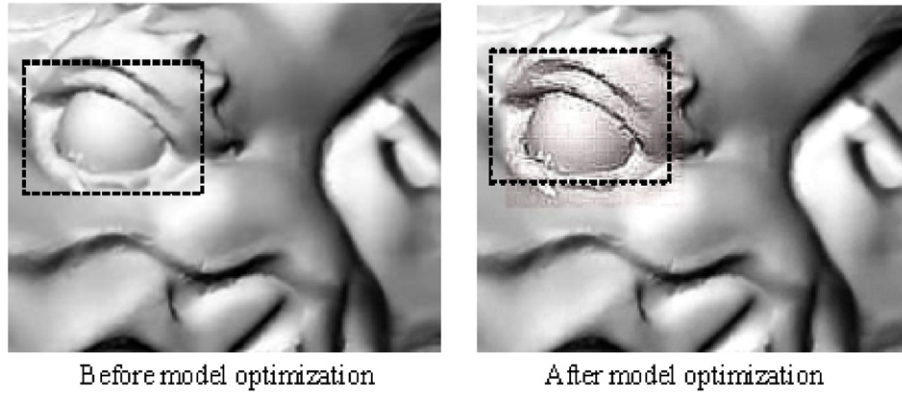


Figure 8. Comparison of visual effects of model optimization.

Table I. Comparison results of plane optimization (unit: cm).

Project	1	2	3	4	5	6	7	8	9	10
Poisson algorithm top	18.3	13.5	14.7	14.1	14.6	13.5	13.2	13.4	13.1	13.1
Poisson algorithm side	18.4	17.6	14.8	12.1	11.2	9.7	9.8	9.1	9.1	9.0
Top of the method in this paper	9.9	9.9	9.7	9.7	9.7	9.7	9.7	9.6	9.6	9.6
The method side of this article	12.5	10.5	9.7	7.5	6.2	5.2	4.8	4.7	2.5	2.1

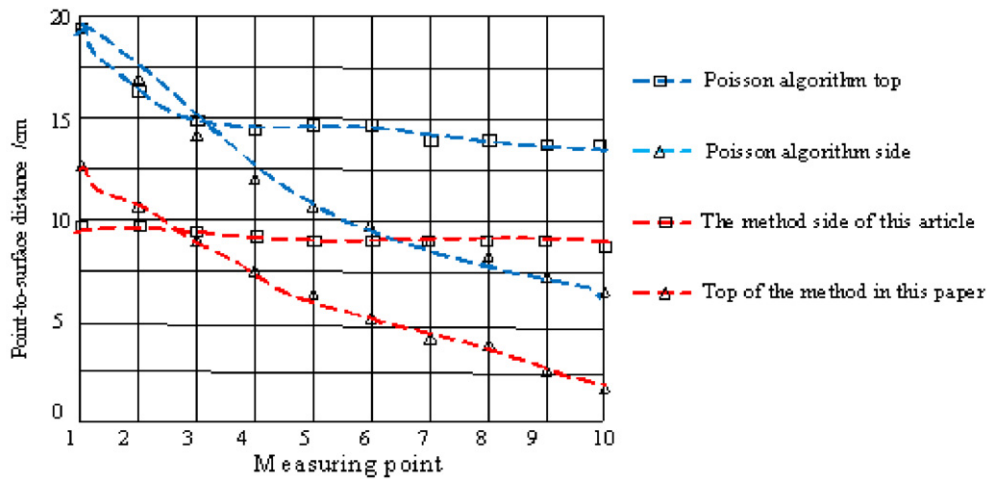


Figure 9. Display results of plane optimization.

Table II. Comparison results of edge optimization (unit: cm).

Project	1	2	3	4	5	6
Poisson algorithm top	0.04	2.45	3.58	4.26	5.24	2.91
Poisson algorithm side	0.07	2.93	4.21	3.75	4.72	3.16
Top of the method in this paper	0.01	5.63	4.86	7.34	6.23	7.39
The method side of this article	0.01	6.01	5.23	4.47	6.38	4.29

Table III. The efficiency of the reconstruction algorithm (unit: min).

Method	Optimization method in this paper	Delaunay triangular mesh surface construction method	Poisson reconstruction method
Time-consumption	25.4	27.2	28.5

triangular mesh surface construction method, and the Poisson reconstruction method, and the time-consumption records and comparisons are made.

The comparison results of Table III are as follows: through the test and comparison of three methods, the time consumption of the optimization method in this paper is 1.8 min, which is lower than that of Delaunay triangular mesh

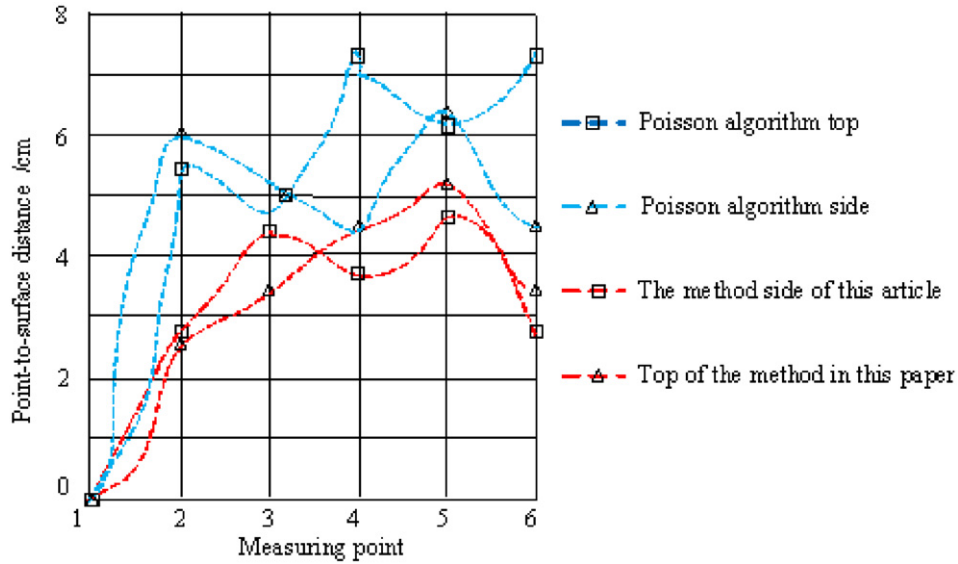


Figure 10. Display results of edge optimization.

surface construction method and 3.1 min, which is lower than that of Poisson reconstruction method. The efficiency is improved by more than 2.5%, which has an obvious effect on the execution efficiency.

#### 8.4 Experimental Analysis

(1) This paper uses high-precision three-dimensional line segments reconstructed from oblique images in various directions as an aid. On the one hand, the points in the same plane are corrected to a reference plane, and the vertices of the triangular mesh in the plane are “smoothed”, so that the model plane conforms to the coplanar characteristics, and the goal of optimizing the visual effect of the model plane is achieved. On the other hand, the points on the same straight line at the edge triangulation are corrected to a reference line, and the vertices on the edge triangulation are “straightened”, so that the edges of the model conform to the collinear characteristics, and the purpose of optimizing the edge visual effect of the model is achieved. Therefore, whether it is horizontal or vertical edges and planes, the method in this paper can obviously eliminate the uneven surface, jagged edges, or insufficient smoothness in the Poisson algorithm reconstruction model. From the overall optimization effect of the model, it can be seen that the surface of the optimized Firecrackers-Dancing Dragon is flat, the edges are sharp and straight, which are consistent with the actual Firecrackers-Dancing Dragon model plane and edge geometry, and conform to the actual characteristics of the Firecrackers-Dancing Dragon plane and edges. It can be seen that the visual effect of the optimized model has been greatly improved.

(2) The method in this paper optimizes the points on the same plane, and assigns the values of the triangle mesh vertices on the plane to the same reference plane. Therefore, the plane of the model optimized by the method in this paper has better flatness, and the points on the plane tend to be

coplanar. It shows that the plane accuracy optimized by the method in this paper is improved by about 50% compared with the Poisson algorithm, and it can reach 0.5 pixels at a resolution of 5 cm. The accuracy of the side of the model is slightly lower than that of the top. This is mainly because the LIDAR data has a weak ability to acquire the side point cloud of the model, which can result in lower accuracy of the side edge. However, it is still higher than the 1-pixel accuracy of the Poisson algorithm. Besides, the standard deviation of the plane distance of the method in this paper is only about 1/8 of the Poisson algorithm, which is generally less than 0.5 cm, and the maximum plane distance is relatively close to the mean value. The Poisson algorithm has a large standard deviation of the plane distance, and the unevenness of the model surface is more serious, and the distribution on both sides of the plane is relatively discrete. The result of the overall error of the model shows that the accuracy of the model optimized by this method is about 0.6 pixels, which is nearly double the 1.1 pixels of Poisson algorithm.

#### 9. CONCLUSION

This paper is based on the line feature-assisted method of Wupaolong point cloud model optimization for craft paper binding. By fitting the datum plane of the paper binding and assisting with high-precision three-dimensional line segments, the surface and edges of the dragon dance are corrected and optimized. The method solves the problem of poor visual effects such as uneven surface and jagged edges of the Firecrackers-Dancing Dragon model based on point cloud construction, and provides new research ideas for the optimization of the object triangulation and the model. This method can accurately realize the 3D modeling of Wupaolong, establish the object 3D data information through the three-dimensional model, realize the unification of production standards, and adjust the simulation posture

of the model, which augments the production process of Wupaolong.

Several key technologies in the technical process of constructing and optimizing the three-dimensional model of the target based on the line feature are studied. However, there are still some issues that have not been considered. Possibility of errors in the positioning of the end points of the line segments with the same name as they may not correspond one to one. Therefore, it is difficult to accurately locate the endpoints of the three-dimensional line segments, and the two three-dimensional line segments produced by the plane intersection method may not be collinear. There is an immediate need to solve the problem that the plane intersection lines are not collinear in the three-dimensional reconstruction of multi-view line features.

## ACKNOWLEDGMENT

The study was supported by “Guangxi philosophy and Social Science Foundation of China (Project No. 20BTY007) and Guangxi Higher Education Undergraduate Teaching Reform Project (Project No. 2021JGA358)”.

## REFERENCES

- <sup>1</sup> R. Chen, S. Han, J. Xu, and H. Su, “Point-based multi-view stereo network,” *Z.* 1538–1547 (2019).
- <sup>2</sup> P. Cang and Z. Yu, “Research on 3D building information extraction and image post-processing based on vehicle LIDAR,” *EURASIP J. Image and Video Processing* **2018** (2018).
- <sup>3</sup> H. Lifang and H. Jian Group, “The law of intangible cultural heritage and economic interaction and its change factors - field investigation based on dance meadi,” *S Border Economy and Culture* **2021**, 47–52.
- <sup>4</sup> H. Lifang and H. Jian Group, “Development trend and innovation strategy of physical infrared cultural heritage in digital economic age - based on binyang dance meal dragon,” *Sport Science and Technology* **42**, 86–88+93 (2021).
- <sup>5</sup> H. Jian Group, “Progress and review of the national intangible cultural heritage dance dragon dragon dragon research,” *Shandong Sports Technology* **39**, 11–16 (2017).
- <sup>6</sup> M. J. Leotta, C. Long, B. Jacquet, M. Zins, D. Lipsa, J. Shan, B. Xu, Z. Li, X. Zhang, S. Chang, M. Purri, J. Xue, and K. Dana, “Urban semantic 3D reconstruction from multiview satellite imagery,” *Proc IEEE Comput. Soc. Conf. Comput. Vis. Pattern Recognit.* (2019).
- <sup>7</sup> X. Gu, Z. Fan, Z. Dai, S. Zhu, F. Tan, and P. Tan, “Cascade cost volume for high-resolution multi-view stereo and stereo Matching,” *2020 IEEE/CVF Conf. on Computer Vision and Pattern Recognition (CVPR)* (IEEE, Piscataway, NY, 2020).
- <sup>8</sup> E. Xiang, Z. Y. Wang, S. S. Lao, and B. C. Zhang, “Pruning multi-view stereo net for efficient 3D reconstruction,” *ISPRS J. Photogramm. Remote Sens.* **168**, 17–27 (2020).
- <sup>9</sup> P. Cang and Z. Yu, “Research on 3D building information extraction and image post-processing based on vehicle LIDAR,” *EURASIP J. Image and Video Processing* **2018**, 1–8 (2018).
- <sup>10</sup> R. Zhang, S. Zhu, T. Fang, and L. Quan, “Distributed very large scale bundle adjustment by global camera consensus,” *Proc. IEEE Int. Conf. Comput. Vis.* (2017).
- <sup>11</sup> L. Perumal, “A new triangular mesh generation technique,” *Int. J. Machine Learning Computing* **5** (2019).
- <sup>12</sup> S. Bhattarai, K. Dahal, P. Vichare, and W. Chen, “Adapted delaunay triangulation method for free-form surface generation from random point clouds for stochastic optimization applications,” *Structural and Multidisciplinary Optimization* **61**, 649–660 (2019).
- <sup>13</sup> J.-D. Favreau, F. Lafarge, A. Bousseau, and A. Auvolat, “Extracting geometric structures in images with Delaunay point processes,” *IEEE Trans. Pattern Anal. Mach. Intell.* **42**, 837–850 (2018).
- <sup>14</sup> X. Jia, X. Huang, F. Zhang, Y. Gao, and C. Yang, “Robust line matching for image sequences based on point correspondences and line mapping,” *IEEE Access* **7**, 39879–39896 (2019).
- <sup>15</sup> Y. Sun, Y. Y. Sun, Q. Wang, K. Tansey, S. Ullah, F. Liu, H. Zhao, and L. Yan, “Multi-constrained optimization method of line segment extraction based on multi-scale image space,” *ISPRS Int. J. Geoinf* **8**, 183 (2019).
- <sup>16</sup> S. Kim and R. Manduchi, “Multi-planar monocular reconstruction of manhattan indoor scenes,” *Proc. IEEE/CVF Int. Conf. Comput. Vis.* 30–33 (2019).
- <sup>17</sup> D. L. Cui and J. W. Leng, “Point-line matching algorithm based on pure geometric line feature matching,” *Computer Appl. Software* **37**, 186–191 (2020).
- <sup>18</sup> Y. Liu, “A fast positioning method for extracting the line features of lidar point clouds,” *Sensors Microsystems* **39**, 34–37 (2020).
- <sup>19</sup> L. Cao, “Fast reconstruction method of building model based on oblique photographic line feature,” *J. Surveying and Mapping Science and Technol.* 531–537 (2015).
- <sup>20</sup> Z. G. Qu and S. Q. Niu, “Research on an improved adaptive weighted median filter algorithm,” *Computer Technol. Development* **28**, 86–90 (2018).
- <sup>21</sup> L. M. Lin and M. Wang, “Improved binocular vision SLAM algorithm for point-line features,” *Computer Measurement and Control* **27**, 156–162 (2019).
- <sup>22</sup> J. X. Wang and W. Y. He, “LBD descriptor and line segment matching under multiple constraints,” *J. Image Graph.* **24**, 237–247 (2019).
- <sup>23</sup> J. J. Sun, Y. Zhao, and S. G. Wang, “SIFT image matching algorithm based on edge information,” *J. Jilin University (Information Science Edition)* **36**, 200–206 (2018).
- <sup>24</sup> C. Li and X. K. Zeng, “Research on the fineness of the three-dimensional model of urban drone tilt photography,” *Surveying and Spatial Geographic Information* **43**, 205–207 (2020).
- <sup>25</sup> J. H. Liu, “Sports industry in the network and digital era,” *Sports Sci.* **39**, 56–64 (2019).
- <sup>26</sup> L. Juan, S. Roi, R. Fdez-Vidal Xose, and M. P. Xose, “Two-view line matching algorithm based on context and appearance in low-textured images,” *Pattern Recognit.* **48**, 2164–2184 (2015).
- <sup>27</sup> B. X. Xie and X. Y. Hu, “Misunderstandings in the application of the theory of ‘stage reality’ in the protection strategy of ethnic tourism culture—Based on the reflection on the Development model of ‘front stage curtain, backstage,’” *Yunnan Social Sciences* 96–103+186 (2019).
- <sup>28</sup> R. B. Han, “Activation, inheritance and innovation of intangible cultural heritage—from the perspective of ‘emotional mechanism,’” *Folklore Res.* 56–66+158 (2019).
- <sup>29</sup> G. Q. Hao, “Research on the network practice and cultural capital of online ‘Kitchen Girls,’” *J. Yunnan Nationalities University (Philosophy and Social Sciences Edition)* **36**, 23–29 (2019).
- <sup>30</sup> M. M. Wang and C. C. Meng, “The interactive mechanism of technological innovation and cultural consumption and its impact on the transformation and upgrading of cultural industries: an analysis based on the perspective of supply-side reform,” *Taxation and Economy* 50–55 (2019).